Mon. Not. R. Astron. Soc. **268**, 953–965 (1994)

Head-on mergers of systems containing gas

F. R. Pearce,[1] P. A. Thomas[1] and H. M. P. Couchman[2]

[1] *Astronomy Centre, MAPS, University of Sussex, Brighton BN1 9QH*

[2] *Department of Astronomy, University of Western Ontario, London, Ontario N6A 3KV, Canada*

Accepted 1994 January 24. Received 1994 January 20; in original form 1993 October 18

ABSTRACT

Several simple head-on mergers between model galaxy clusters containing a mixture of gas and dark matter are examined, testing the coupling of the gas to the underlying collisionless material. The gas is shocked, irreversibly dissipating the energy fed into it by the collisionless component, and forms a resolved constant-density core. For the dark matter, however, admixture of phase-space vacuum is not very efficient and a constant-density core is not produced. In the final state the central gas has little residual disordered kinetic energy, indicating that small-scale streaming motions do not help to support the gas.

Key words: shock waves – methods: numerical – galaxies: clustering – galaxies: formation – intergalactic medium – dark matter.

1 INTRODUCTION

In this paper we examine the behaviour of the intracluster medium in galaxy clusters. Cluster gas is important because it is the dominant form of baryonic matter in these objects and observations of its X-ray emission provide some of the best currently available constraints on cluster properties. The gas has temperatures in the region of 5×10^7 K and emits mainly via thermal bremsstrahlung. This emission is observed in the X-ray waveband, where galaxy clusters form some of the brightest sources. As bremsstrahlung emission depends upon the *square* of the gas density it is very sensitive to this parameter, and so the surface brightness is sharply peaked towards the central regions. Much debate has centred around the observation of a constant-density central region in most clusters (Jones & Forman 1984) and the relevance of this when choosing a profile for the underlying dark matter. We examine the merging scenario to show that constant-density gas cores form naturally *without* a similar core in the dark matter. The question of whether the gas attains the virial temperature is also investigated. Previous simulations (Evrard 1990, hereafter E90; Thomas & Couchman 1992, hereafter TC92) suggested that it may not – with partial support being provided by residual small-scale streaming motions. We find no evidence for this, but preliminary results from off-centre mergers suggest that a large fraction of the gas energy can be provided by large-scale ordered motion (i.e. rotation).

Early attempts to study the behaviour of gas in an astrophysical context were pioneered by Larson (1978) and extended by Cavaliere et al. (1986), who used a hydrostatic approximation to model the gas. This is possible since the high temperatures imply high sound speeds, which should allow the gas to adapt rapidly to any global changes in the potential. More recently, attempts have been made to treat the gas more physically by letting it convert into stars when a certain condition related to the local density and temperature is reached (Carlberg 1986).

The development of more sophisticated gas codes (such as SPH), which were able to handle large density contrasts, has enabled several groups to carry out large simulations modelling cluster-scale sections of the Universe (E90; TC92; Hernquist & Katz 1989; Cen et al. 1990; Katz & White 1993, amongst others). Usually the largest object in the simulated volume is identified with a galaxy cluster and studied in detail. The formation history of this object is often confused because of the complicated initial state. More recently, Navarro & White (1993) have looked at simple mergers and have also studied the effect of changing the particle number. They have shown that SPH is a remarkably robust technique which gives 'broad brush' results for collapses with only 350 particles per cloud. In this paper we intend to study the collision mechanism in detail, for which we require greater resolution. We find that more than 1000 gas particles per cloud are required to model the collision process accurately.

We intend to adopt the approach of simplifying the problem until we can hope to understand the physics. To achieve this we abandon all pretence of modelling a definite cosmology, considering objects similar to those studied in detail in Pearce, Thomas & Couchman (1993, hereafter Paper I), where purely collisionless systems were examined. We build upon the ground-work laid there by introducing a gaseous component that makes up 11 per cent of the cluster by mass. The exact amount is not important although observed clusters do contain about this much gas (see Sarazin 1986 for a general

review of cluster properties, and Fabian 1991). By comparing simulations both with and without a gas component, we hope to gain an insight into the physics of the combined system.

Inclusion of gas in a simulation allows a more direct comparison with observed phenomena. This is because in the real world dark matter has not yet been observed directly, so any simulation containing purely dark matter must be related to the world we see in some way, a process that requires additional assumptions to be made. As our model contains both dark matter and gaseous phases, we can hope to check the accuracy of this reasoning.

We collide two subclusters, each made up of a mixture of collisionless (hereafter dark matter) particles and gas. The ratio, β, between the kinetic energy of the dark matter and the thermal energy of the gas is set equal to unity initially. Then

$$\beta = \frac{\sigma^2}{k_B T/\mu m_H} \tag{1}$$

where σ is the one-dimensional velocity dispersion of the dark matter, T is the gas temperature and k_B, μ and m_H are Boltzmann's constant, the relative molecular mass and the mass of a hydrogen atom respectively.

In all our runs we merge two equal-sized objects head-on at different speeds (off-centre mergers will be considered in a future paper (Pearce, Thomas & Couchman 1994)). We show that the gas is shocked, especially in the centre of the cluster where its entropy is increased above that of the equivalent measure in the dark matter. No gas remains with a low enough entropy to sit at the bottom of the potential well formed by the dark matter, and so a core region of constant-density, nearly constant-temperature gas forms. This region is supported almost entirely by thermal pressure, with little residual kinetic motion, and is in hydrostatic equilibrium. In this region the gas is hotter than the dark matter, producing values of $\beta \sim 0.8$. (A value of $\beta < 1$ is consistent with the gas being the more extended component.) Beyond the gas core the two phases have very similar profiles that are close to those obtained in our earlier work (Paper I). This would indicate that the gas can closely follow the dark matter profile in the outer regions.

In this paper we are particularly interested in the central regions of the merger product. A constant-density core region never forms in the dark matter, confirming the results of Paper I. For a purely gaseous collision a small core region forms, due to the shock of dissipating the collisional kinetic energy. In the combination gas and dark matter runs, however, a larger core forms because, in addition to the initial shock, energy is exchanged between the two phases whilst they are separated, and this becomes irreversibly tied to the gas when it is shocked again by a secondary merger. It is the combination of energy feed into the gas and the irreversible jump in entropy that increases the size of the core region visible in the gas.

In the following section we explain the computational methods used in more detail and give the specific parameters and configuration of each of our five mergers. In Section 3 we present the results, with Section 4 containing a discussion of them. We present our conclusions in Section 5.

2 METHOD

2.1 Computational algorithm

The majority of the simulations in this paper were carried out using a combination of smoothed particle hydrodynamics (SPH) to follow the gas and an adaptive particle-particle, particle-mesh (AdP^{3}M) technique to handle the gravity. We call this hybrid code AdP^{3}M-SPH.

AdP^{3}M-SPH is the version of Hugh Couchman's AdP^{3}M (Couchman 1991) used by Paper I with gas forces applied at the particle-particle level. SPH was introduced by Lucy (1977) and Gingold & Monaghan (1977) who used it to model polytropic stars. As in Paper I we use isolated boundary conditions in all the simulations presented here.

We use an SPH implementation similar to that of Monaghan, for which the formalism has been published several times (Gingold & Monaghan 1982; Hernquist & Katz 1989; Monaghan 1992). When merging SPH and AdP^{3}M the only difficulty arises when a particles smoothing kernel extends over a subgrid boundary (subgrids are positioned by the AdP^{3}M algorithm so that more mesh points are placed in the denser regions. This reduces the number of particle-particle calculations that need to be carried out). We handle this case by checking if a particle has a neighbour outside the subgrid. If it does then the SPH forces are applied at the coarser level. A full description and details of the tests can be found in Pearce (1992) and Couchman, Thomas & Pearce (hereafter CTP, in preparation). Some general remarks concerning the implementation of SPH can be found in Martin, Pearce & Thomas (1993, hereafter MPT).

2.2 Initial conditions

We carried out five main runs, the parameters for which are listed in Table 1. All involved colliding two equal-mass clusters at different speeds. Each merger was begun with the two spherically symmetric clusters just in contact. The collision speed of run dg1.0 was set equal to the circular speed at the edge of one of the clusters. This is approximately half the one-dimensional virial speed at the centre of the cluster. It is also roughly equivalent to the sound speed in the outer regions. This run is very similar to run f3 of Paper I, which here we call run d1.0 for consistency of notation as it contains only dark matter. We include the parameters in Table 1 for comparison, as both had the same total mass and collision speed. The third and fourth runs, dg2.0 and dg0.5, had collision speeds twice and half that of run dg1.0 respectively. The final run, g1.0, was carried out at the same speed as run dg1.0 but contained only gas.

The systems we model have initial Hubble density profiles of slope 3:

$$\rho = \rho_c \left[1 + \left(\frac{r}{r_c}\right)^2\right]^{-\frac{3}{2}} \tag{2}$$

within some outer radius R_{max}, $\rho = 0$ beyond R_{max}. Here ρ_c is the central density and r_c is the cluster core radius.

The core radius needs to be well within the outer boundary but large enough so that we can detect a reduction during mergers. We compromise on $R_{max}/r_c = 16$. The gravitational softening, s, was fixed at $s = 0.4r_c$, above the interparticle

separation in the original cores. This is explained in greater detail in Paper I.

Each phase in each of the initial clusters contained 8192 particles, giving 32 768 particles in all (except for the single-component runs, d1.0 and g1.0, which had half this number). With each gas particle having $\frac{1}{8}$ of the mass of a dark matter particle, the latter component dominates the overall potential.

The timestep, Δt, in our simulations is fixed by the condition

$$\Delta t = 0.25 \min_i \left(\frac{d}{a_i} \right)^{\frac{1}{2}}, \tag{3}$$

where a_i is the acceleration on particle i. d is a distance for which we take

$$d = \min(s, h_{\min}) \tag{4}$$

where $h_{\min}$ is the minimum smoothing length found by the SPH algorithm (i.e. it is controlled by the greatest density currently in the simulation). In practice $s > h_{\min}$ at all times for our models, and so we are applying a more restrictive timestepping criterion than that used in Paper I. Too long a timestep leads to spurious jumps in a gas particle's entropy because close interactions are not accurately followed. This is not a problem in our simulations – see Fig. 4 and the discussion in the following section.

The gas is positioned by transforming a relaxed uniform box into the desired density profile. This ensures that the initial gas separations are close to a relaxed state immediately. The particles within the initial box are ordered in radius from an arbitrary centre and then this radius is adjusted so as to reproduce the density profile. The local density is set from equation (2), whilst the temperature is set equal to σ^2 (i.e. $\beta = 1$). The velocity dispersion, σ, is derived by solving the Jeans equation for the above density profile with no outer cut-off (equation 4-54, Binney & Tremaine 1987). The initial positions of the dark matter are set equal to the gas positions reflected through the centre of each cluster. In Paper I the initial velocities were set equal to the velocity dispersion at the particle's position. This process only spans five of the six phase-space dimensions. In this paper the velocities of the dark matter are drawn from a Gaussian distribution of width σ, fully spanning the available phase space. This change makes no discernible difference to the results. The gas is initially at rest.

2.3 Tests

Tests of the individual codes involved have been published elsewhere (see Paper I for tests of AdP^{3}M, and TC92). We tested our version of SPH by reproducing standard shock results in a 2d by 1d tube. Detailed tests of our SPH implementation are given in MPT and CTP. The correct jump conditions were reproduced with a shock front that was about 6 particles deep. This would indicate that over 1000 particles are required to model a three-dimensional shock correctly. To test this we have carried out collisions with 128 and 1024 gas and dark matter particles in each object, for comparison with our main runs which contain 8096 particles. The 128-particle mergers do not have the resolution to model the structure of the halo, and give very different results. The 1024-particle run gives a reasonable radial structure not too dissimilar from the full run, but it is only when we go to 8096 particles that the energy transfer between the dark matter and the gas is accurately modelled and the core structure of the merger product is correctly resolved. A detailed comparison between these runs and the main one is given in Section 3.4 below.

A quick and revealing method of looking at global changes in the system is an energy track. This is illustrated later by Fig. 9, which shows the energy statistics for one of our mergers. Energy and time are normalized by setting the total mass, $M_{\rm tot}$, the outer radius of the system, $R_{\max}$, and G equal to unity. The thermal energy is displayed multiplied by a factor of 8, as the total gas mass is $\frac{1}{8}$ that of the dark matter. The effect of the merger is clearly visible in Fig. 9, although it is impossible to judge the accuracy of the energy conservation due to the scaling. Fig. 1 expands the system total energy and scales it to the initial value. There are nearly 1000 timesteps in this plot, with typical energy conservation better than 1 part in 10 000 per step. The same accuracy, smoothing and timestepping parameters were used in all of the runs detailed in this paper.

The combined code was tested by observing the evolution of a static configuration. A single isolated cluster was set up following the prescription given above. This consisted of 8192 gas and 8192 dark matter particles in what should be a nearly stable arrangement. For this run the total energy is conserved to better than 0.4 per cent and the start and finish parameters are listed in Table 1. Some expansion at the edge is to be expected as here the gas is not in pressure balance. As in our previous paper (PTC) the choice of centre is very important when plotting logarithmic density profiles. For the static run we tried the 'true' centre (the position about which the initial profile was built), the position of the gas particle with the highest local density, the mean position of the 100 or so densest gas particles, the position of the most tightly bound dark matter particle and the mean position of the 100 or so most tightly bound particles. All five of these positions remained close together, within less than the gravitational softening length. In what follows, the mean position of the 100 or so densest gas particles is used as the expansion centre for profiling and radial measurements.

Fig. 2 shows the initial and final density profiles for the gas and the dark matter, with the end-state taken after approximately the same length of time as the collisions discussed below. The expansion of the edge can readily be seen, as can a very small increase in the core size of both the gas and the dark matter. Some rearrangement in the centre is almost certain to occur, as the existence of a gravitational softening length is not taken into account when setting up the profiles. This effect will be most noticeable in the densest regions, particularly so for the gas, as the same particles remain in the centre whilst the dark matter particles in the region keep changing. Some small rearrangement is inevitable anyway, as this distribution function is not formally static. The small changes in the core parameters occur quickly and then stop, with the system rapidly settling into a steady state almost indistinguishable from the initial conditions.

The evolution of the gas temperature profile is shown in Fig. 3, along with the maximum and minimum temperatures of particles in each radial bin at the end-point. Some cooling has taken place in the outer regions due to the expansion. This has occurred almost isentropically. A plot of initial radius against

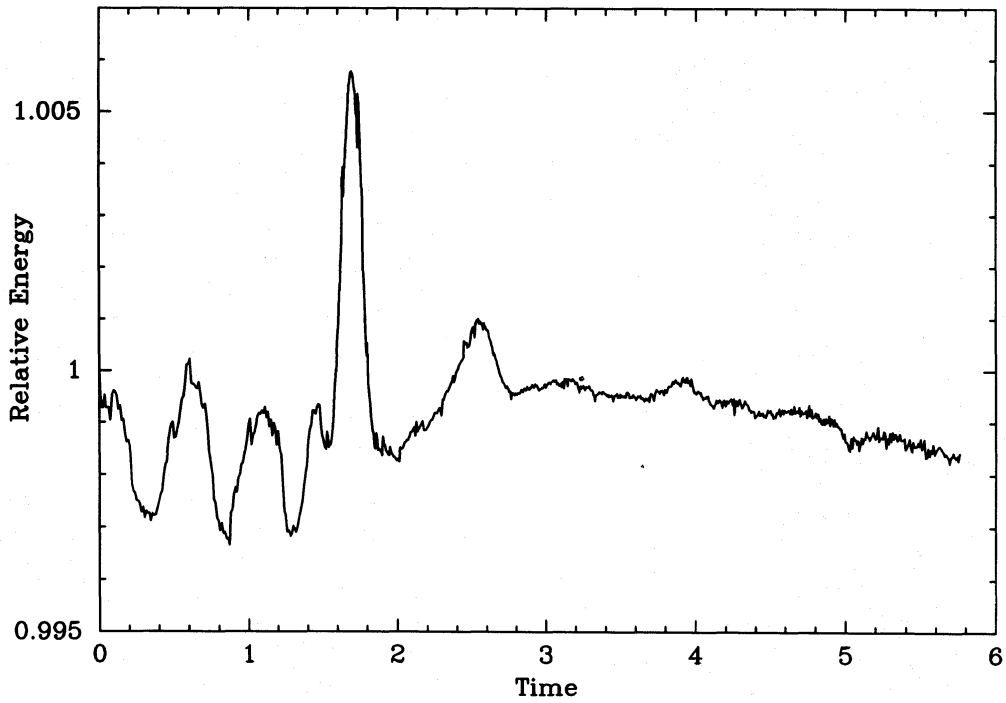

Figure 1. Energy conservation.

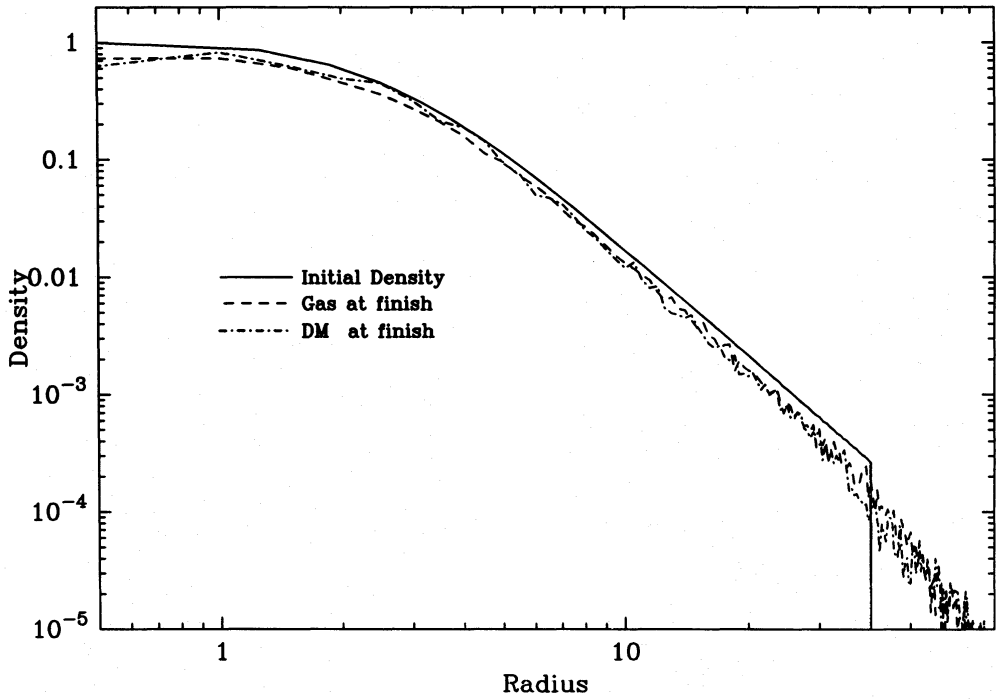

Figure 2. Evolution of the gas and dark matter density profiles.

entropy change is given in Fig. 4. The entropy change ΔS is defined as

$$\Delta S = \log_{10}\left[\frac{T_b \rho_a^{\frac{2}{3}}}{T_a \rho_b^{\frac{2}{3}}}\right] \tag{5}$$

where T and ρ are the temperature and density of a particle and the subscripts a and b refer to the start and finish times respectively.

The gas has a tendency to order itself in entropy, with low-entropy gas sinking to the bottom of the potential well whilst high-entropy gas floats. It is therefore vitally important to keep the scatter in entropy produced by the algorithm (the width in Fig. 4) as small as possible, otherwise artificial cool core regions can arise.

The slight upward drift in the mean of Fig. 4 arises for a variety of reasons. First, the density is overestimated at the first step because the initial configuration is not completely relaxed,

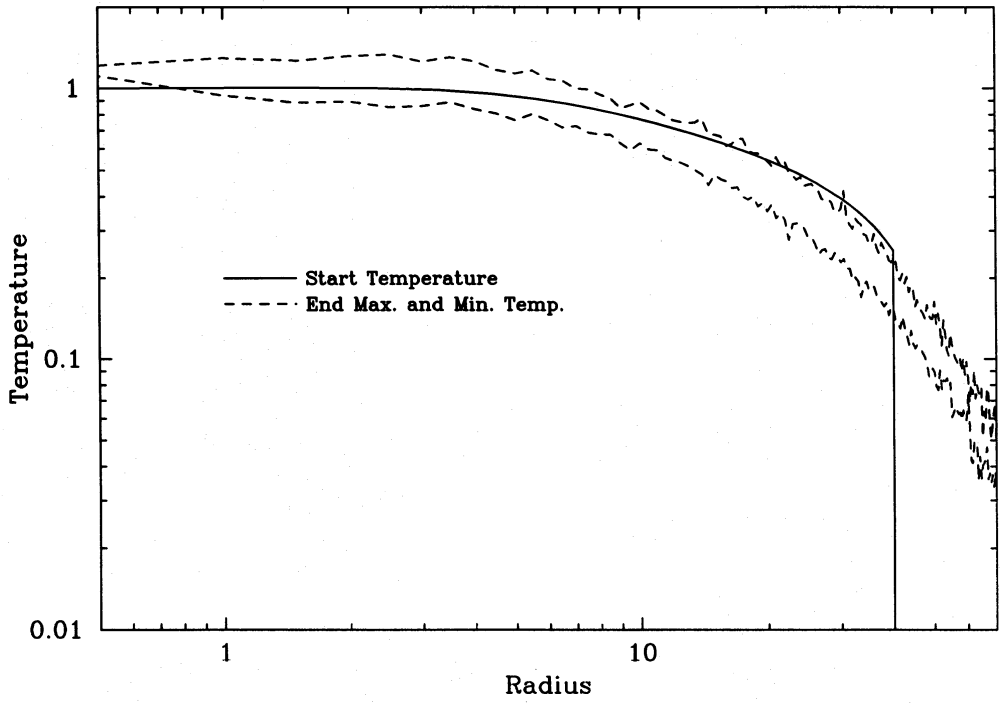

Figure 3. Evolution of the gas temperature and the range in temperatures at the end-point.

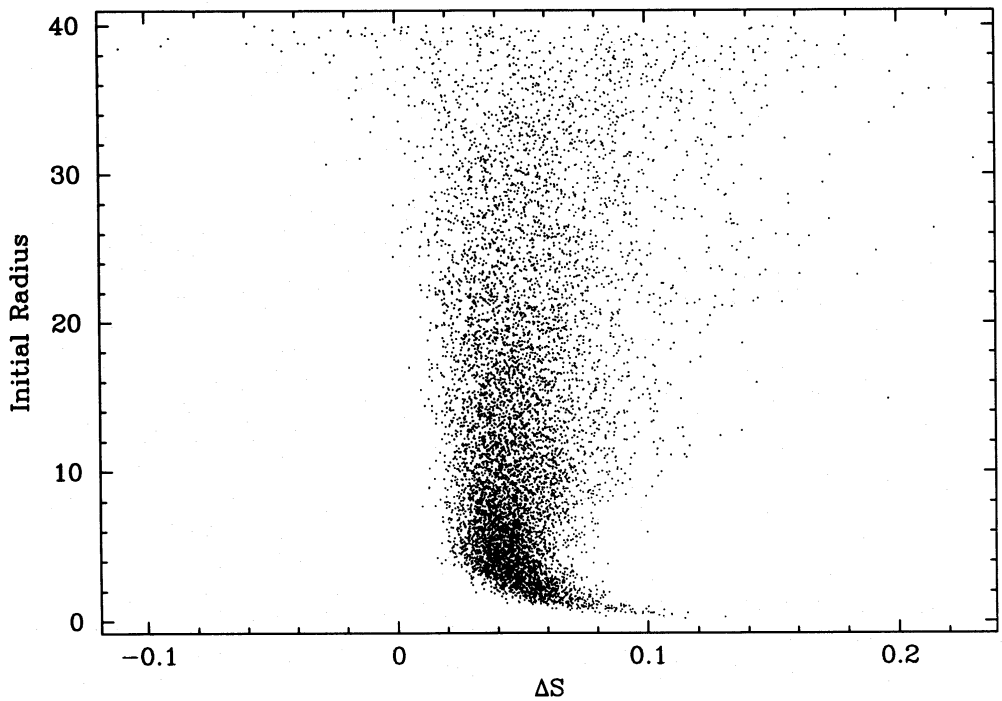

Figure 4. Entropy change in a static model.

which leads to an underestimate of the initial entropy. As the gas relaxes back to a stable configuration the SPH density returns to the 'correct' value. This relaxation is artificial and not due to any actual density change, and so a slight jump in entropy occurs. Secondly, any application of the artificial viscosity, which contains sub-sonic terms, will increase the entropy of the particles, so we expect a slow upward drift. The jumps in a gas particle's entropy due to collisional shocks are over an order of magnitude greater than these effects.

3 RESULTS

3.1 Dark matter only

The merger of purely collisionless systems has been discussed in detail in Paper I. We reiterate the general results here for completeness.

During the merger of two systems of collisionless material the two dark matter spheres approach and overlap, and then the core regions clearly reseparate before turning around and

Table 1. Run parameters, by column the run label, the number of particles in each phase, the ratio of the collision speed to the central velocity dispersion, the best-fitting core radii (in units of the gravitational softening length) and the best-fitting slopes.

Label	N_{DM}	N_{gas}	V_{coll}/σ_0	a_{DM}	a_{gas}	s_{DM}	s_{gas}
dg0.5	2×8192	2×8192	0.25	2.20	3.46	2.80	2.96
dg1.0	2×8192	2×8192	0.5	2.36	3.51	3.08	3.01
dg2.0	2×8192	2×8192	1.0	2.10	4.56	2.82	2.81
g1.0	0	2×8192	0.5	-	3.27	-	3.18
d1.0	2×8192	0	0.5	2.22	-	2.82	-
single_{end}	8192	8192	0	2.85	3.01	3.36	3.24
single_{init}	8192	8192	0	2.50	2.50	3.00	3.00
dg4096	2×1024	2×1024	0.5	2.13	3.92	3.02	2.74
dg512	2×128	2×128	0.5	7.60	26.8	3.94	4.40

falling back in again. The amplitude of the core separation rapidly decreases, with two 'bounces' being clearly visible on an energy plot.

The final density profile is close to $\rho \propto r^{-3}$ in the outer regions, and the size of the original constant-density core region drops by almost the maximum amount allowable by phase-space constraints. This would indicate that no large-scale constant-density core region should exist in the dark matter (and potential well and mass) profiles of observable objects. (Note, however, that these models ignore the influence of a central galaxy, which may sweep the core free of dark matter via two-body interactions.)

In Fig. 5 we give the potential energy tracks for this run (d1.0), the pure gas run (g1.0) and the combination gas and dark matter run carried out at this collision speed (dg1.0).

The final density profiles for both this pure dark matter run and the pure gas run (g1.0) mentioned below are shown in Fig. 6.

3.2 Gas only

The merger of two purely gaseous spheres is in effect the simplest of all the five runs considered here. During the collision the forward side of each of the spheres is compressed, forming an enhanced-density slab perpendicular to the collision axis. The isotropic nature of the gas forces rapidly destroys this structure in favour of a spherically symmetric density profile. In the final state the original gas spheres form two hemispheres aligned along the collision axis, with little interpenetration occurring. Only one deepening of the potential is seen in Fig. 5 and there are no post-merger oscillations.

The speed with which a spherically symmetric structure is obtained is quite surprising, with the density enhancement along the collision front being smoothed out over a period close to that for local sound crossing. The only signs of a recent merger event are a temperature enhancement and two approximately planar shock fronts propagating outwards perpendicular to the collision axis.

The final static structure has the density profile shown in Fig. 6. This is close to the purely dark matter case, with only a small constant-density core region forming and a slope close to $\rho \propto r^{-3}$ in the outer regions.

To aid in analysing the merger, we binned the gas particles into four groups depending upon their initial positions. The inner 25 per cent by mass we refer to as the core gas, whilst the outer 25 per cent forms the halo gas. There are also two intermediate bins comprising the gas between 25 per cent and 50 per cent (1/2 gas) and between 50 per cent and 75 per cent (3/4 gas). Each bin contains 4000 gas particles with the outer 192 from each initial cluster being ignored for this part of the analysis. There is little mixing between the four groups, with original halo gas remaining, on the whole, as halo gas and original core gas remaining as core gas.

In Fig. 7 we show how the kinetic and total energies of the core gas vary with time. The only significant feature appears as the two cores merge. The kinetic energy picked up during the approach is thermalized, leaving the gas almost stationary. This sudden stop is also seen in the entropy curve plotted above (and in Fig. 8). The core gas loses energy during the collision because it does work on the gas immediately surrounding it. A shock wave propagates outwards, progressively doing work on gas further and further out. The halo gas is given a significant amount of energy by this process, becoming unbound in our case.

The gas is shocked by the collision, with a small constant-density core forming. Fig. 8 shows the entropies of each of the four gas bins plotted against time and scaled to their initial values. The shock of the collision can clearly be seen, along with the large boost in entropy which the halo gas undergoes as it is shocked by gas interior to it. The entropy jump is smallest for the core gas in this case. This will contrast with the mixed runs which we discuss next.

3.3 Dark matter and gas

We have carried out three combination dark matter and gas runs. The main one had the same collision speed as the pure dark matter and pure gas runs discussed above. This run was bracketed by runs at half and twice this speed. The slowest run corresponds to two clusters forming almost in contact, whilst the fastest run is only bound because of the internal energy of the clusters. The central speed would be obtained by two point masses starting from rest at an initial separation of 4 times the maximum radius of one of the clusters. In all three cases the general scenario is the same. The merger follows a path similar to the purely collisionless case until maximum compression is reached. The two gas spheres collide and form a pancake-like structure about the centre of mass of the system, with the short axis aligned with the collision direction. The dark matter component continues on, leaving its original gas behind. At this point the gas is at rest around the centre of mass of the system, whilst the collisionless material has reseparated as in the pure dark matter case discussed above. The two dark matter centres are clearly distinct and some distance from the centre of mass. The central gas is no longer confined in a deep potential well so it expands, falling back towards the nearest

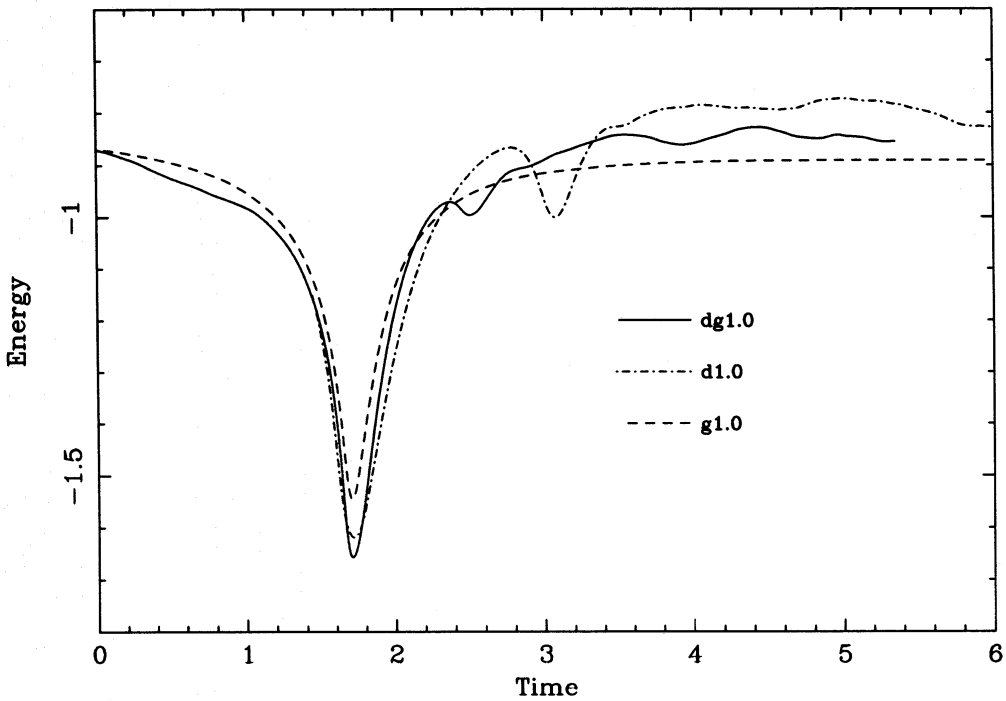

Figure 5. Potential energy for runs d1.0, g1.0 and dg1.0, scaled as in Fig. 9.

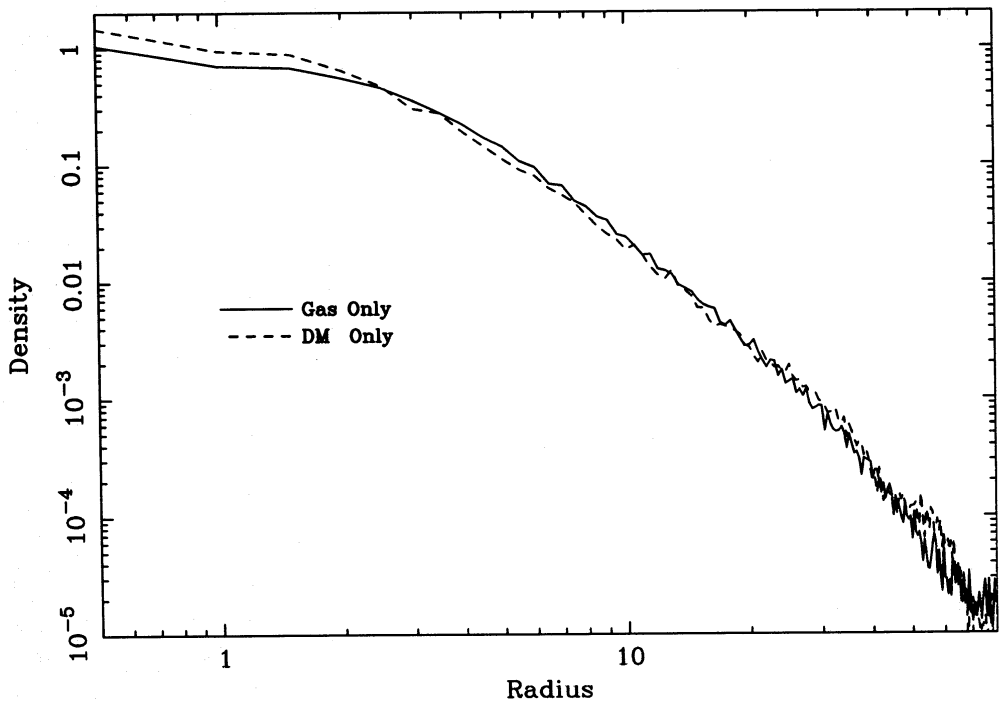

Figure 6. Density profiles from runs d1.0 and g1.0. The densities are scaled so that the initial central density is unity.

receding dark matter sphere (which in the head-on case is not the one from which it started).

As with the collisionless mergers, the simplest way to follow the large-scale evolution of the system is an energy plot. Fig. 9 shows the total energy, the total kinetic and potential energy and eight times the thermal energy of the gas for run dg1.0. Two passages are clearly visible, although only the first of these has a significant impact on the total thermal energy of the gas. The system was allowed to settle down for several crossing times before the steady-state properties of the final object were examined.

A comparison of the potential energy plots for this run, a similar run without gas (d1.0) and a purely gaseous run (g1.0) was given in Fig. 5. The presence of even a small amount of gas causes faster evolution towards the final state after the initial merger event has taken place. This is because each cluster deposits its gas at the centre of mass on the first collision and then this mass drags back the receding dark

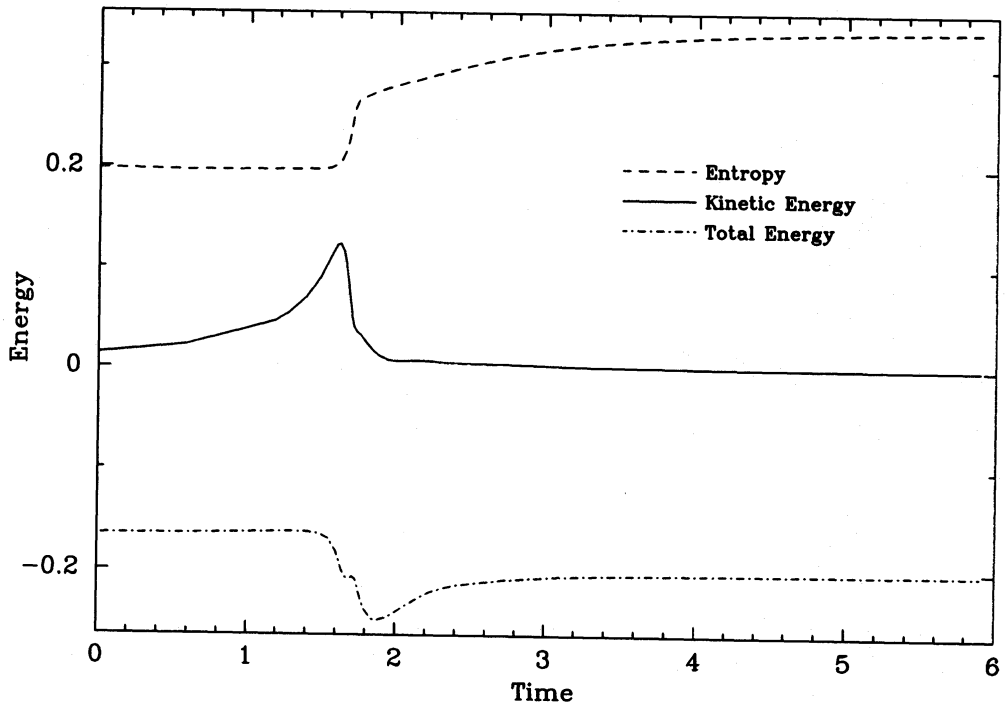

Figure 7. Entropy, kinetic energy and total energy of the core gas. The entropy is scaled arbitrarily whilst the energies are scaled as in Fig. 9.

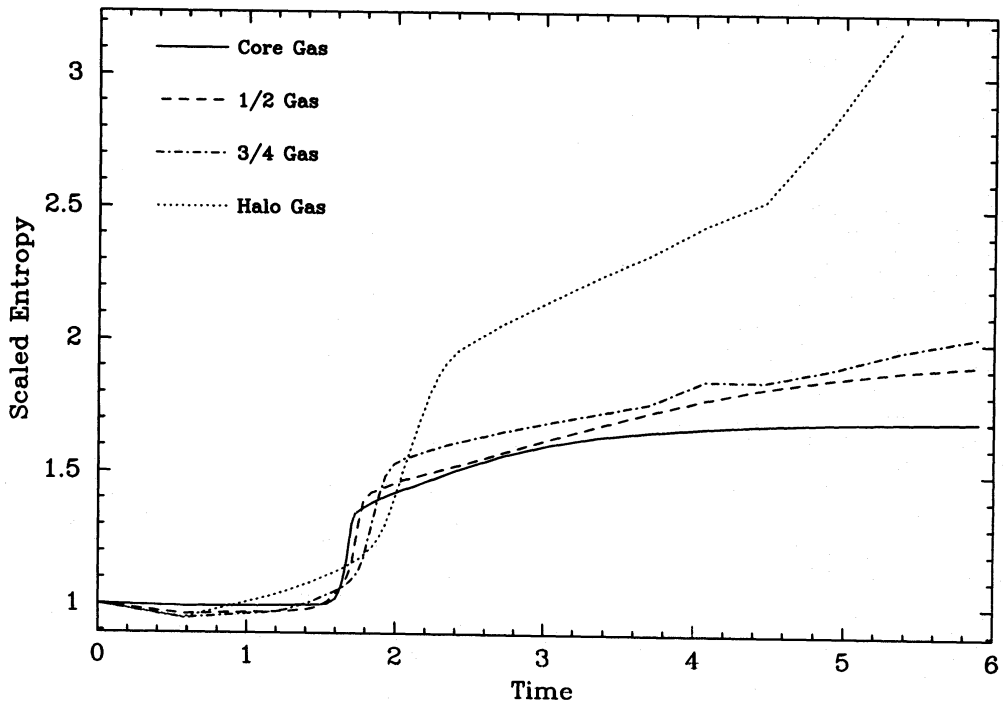

Figure 8. Entropy track for the gas binned by initial radius.

matter components. The time gap between the first and second passages through the centre of mass is significantly reduced in this way. While the gaseous and collisionless components are well separated, energy is exchanged between them.

The density profiles for the gas and dark matter at the end of run dg1.0 are given in Fig. 10. The gas is in hydrostatic equilibrium, and the profiles have stopped evolving. In this combination run the two phases no longer have the same profile, with a definite constant-density core appearing in the gas. Contrast this evolution with the static model of Fig. 2, where the two phases stay closely linked.

Again, as for the purely gaseous case, we bin the gas depending upon its position in the original clusters. Initially similar behaviour is observed, although comparison of Fig. 11 with Fig. 7 reveals that extra structure appears after the first merger. Once the core gas has been halted in a shock and undergone an entropy jump, energy is pumped into it from the receding dark matter. The gas is not confined at the centre

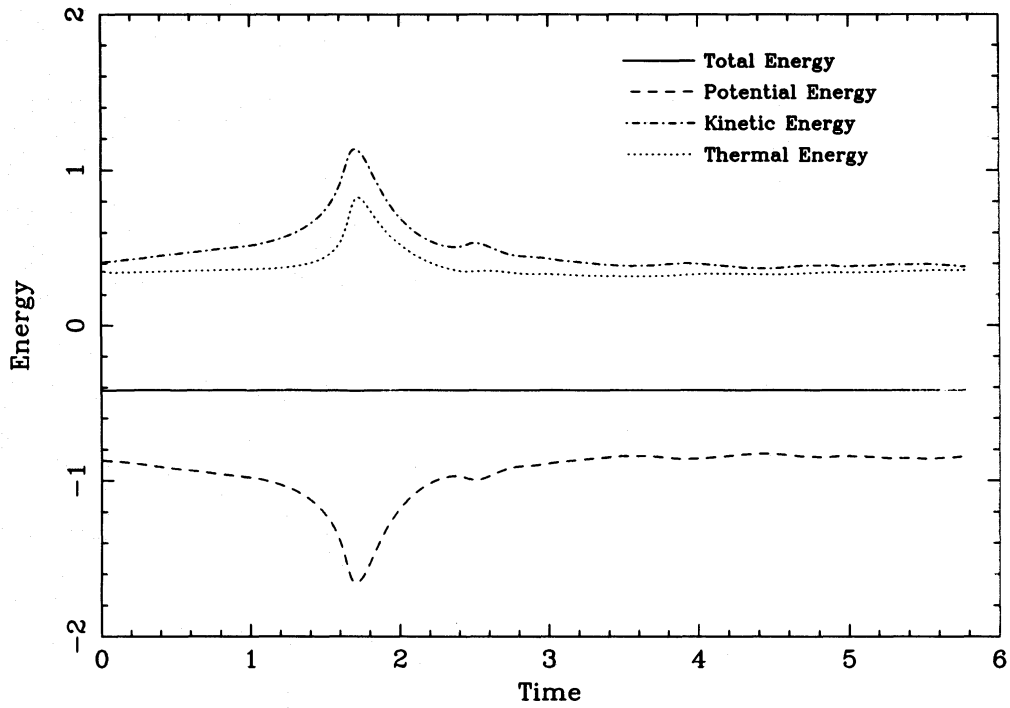

Figure 9. Energy plot from the dg1.0 merger. The energy is in units of the total initial mass, the maximum radius of one of the initial clusters (R_{max}) and $G = 1$. The time unit is taken to be $(R_{max}^3/GM)^{\frac{1}{2}}$.

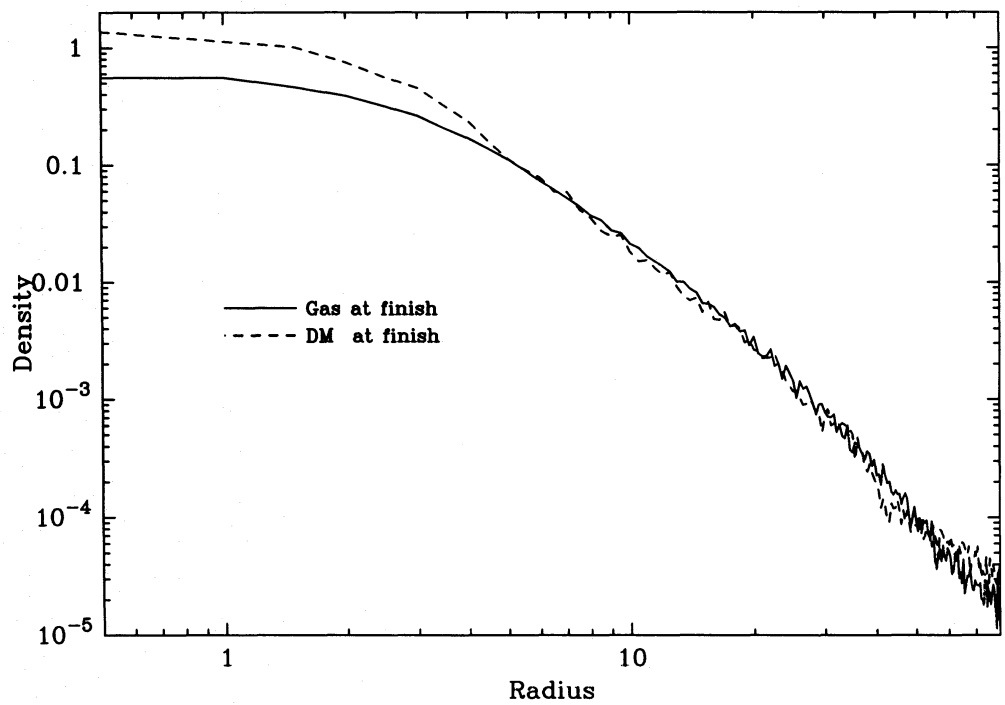

Figure 10. Density profiles for the gas and dark matter at the end of run dg1.0. The densities are scaled so that the initial central density is unity. The gas density has been multiplied by 8, scaling it up to match the dark matter.

of the system and so expands, falling back into the dark matter potential wells. The net effect is to transfer the orbital energy of the dark matter into kinetic energy of the gas. The dark matter spheres do not reach the same separation as in the purely collisionless state, clearly showing that some orbital energy has been lost to the gas.

The main additional feature in Fig. 11 that is not in Fig. 7 is the boost in entropy experienced by the core gas during a second collision. Upon turnaround and re-collapse the core gas, which has gained energy from the dark matter, is heavily shocked, irreversibly increasing its entropy. This second shock is clearly visible in Fig. 12, where the entropy of the gas in run dg1.0 is plotted against time (again relative to the initial values). Only the core gas experiences this strong second shock

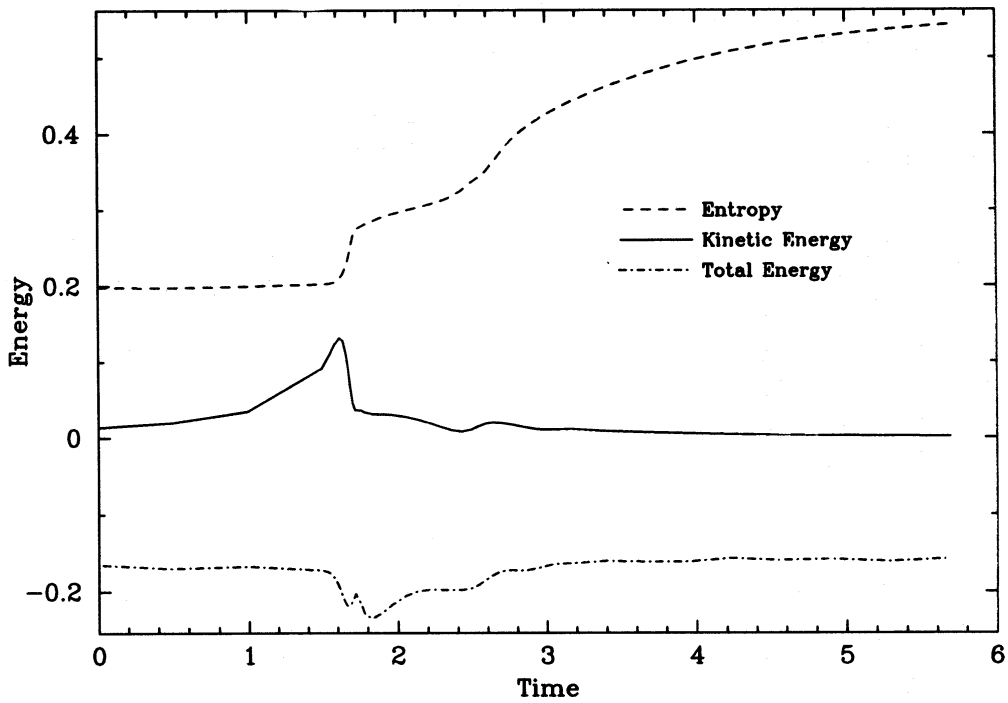

Figure 11. Entropy, kinetic energy and total energy of the core gas from the combined run. Again the entropy is scaled arbitrarily whilst the energies are scaled as in Fig. 9.

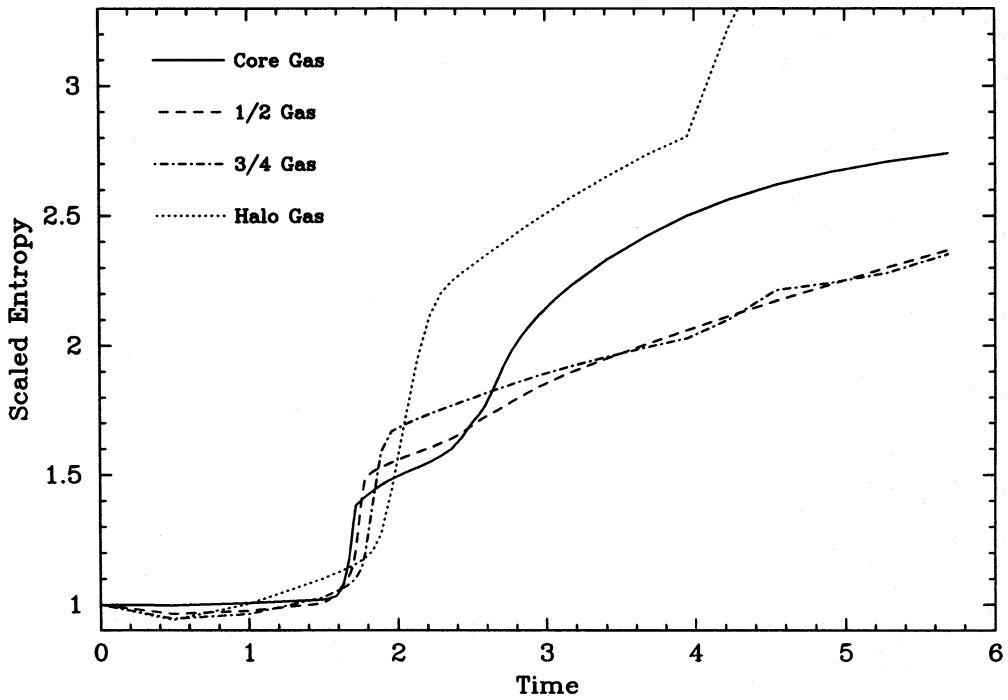

Figure 12. Entropy track for the gas in the combined run binned by initial radius.

as only it undergoes a second collision. The entropy of the core gas is raised to such an extent that no low-entropy gas remains that is capable of sitting at the bottom of the potential well now formed by the dark matter. In this case the core gas has been more heavily shocked than the gas surrounding it but remains at lower entropy. During the run-out period the potential well oscillates slightly as shell-like features in the dark matter are smoothed out. This process causes gas motion which, when dissipated, raises the mean gas entropy at late times.

The final temperature profile is given in Fig. 13. The lack of single particles far from the mean in any bin is an indication of the reliability of the results. (Spurious cooling, an artefact of misconceptions in the application of SPH, can lead to cold particles which sink because of their low entropy, producing an artificial cool region at the centre. The existence

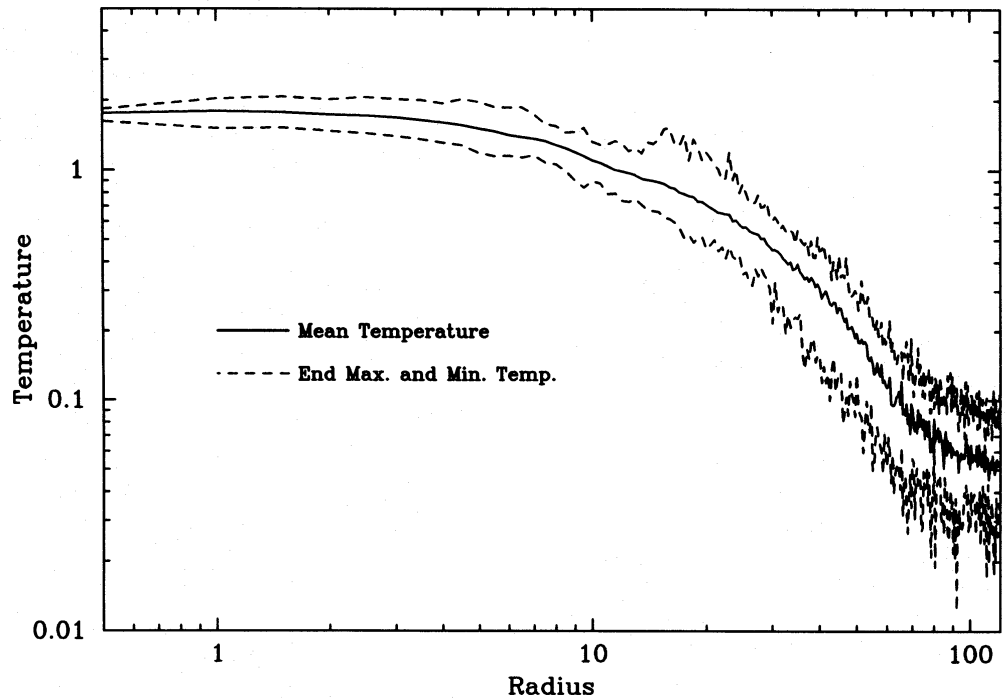

Figure 13. Temperature profile at the end of run dg1.0.

of these particles is masked when only the mean temperature is plotted.) The temperature profile is nearly isothermal in the central region, slowly rolling off beyond the gas core radius. We find no evidence for a central temperature inversion found by previous authors (E90; TC92).

The gas at the end of our simulation has very little residual kinetic energy. The ratio of core gas kinetic to thermal energy is about 4 per cent imediately after the merger, dropping to 1.65 per cent by the end due to the viscous terms in the code. These values are lower than those presented by previous studies (E90; TC92). However, our mergers are head-on with no net angular momentum. Preliminary results from off-centre mergers indicate that as much as 30 per cent of the total energy may be kinetic, due to large-scale rotation of the final state. However, small-scale, random motions in the gas are negligible. They appear to be numerical in origin and become relatively larger when fewer particles are used.

The results for both the faster and slower collisions, runs dg2.0 and dg0.5, are very similar to those presented above. In both the dark matter core size drops whilst a constant-density gas core appears. The final gas core is larger in run dg2.0 than in run dg1.0, whilst for run dg0.5 it is smaller. This is to be expected, as during faster mergers the initial shock is greater and the gas picks up more kinetic energy before the second collsion of the cores. Table 1 lists the measured core sizes for both the dark matter and gas phases for all five of the runs presented above. In all cases the fit was carried out between radii of 2 and 30 gravitational softening lengths with a Hubble density profile of the form

$$\rho = \rho_c \left[1 + \left(\frac{r}{r_c}\right)^2\right]^{-\frac{s}{2}}, \qquad (6)$$

which is similar to equation (2) except that we now have a variable slope, s (instead of fixing $s = 3$). The best-fitting value for s is also listed in Table 1.

The existence of a gas core radius *does not* reveal a similar dark matter core, whereas at larger radii the gas and dark matter do appear to have very similar profiles.

3.4 Effects of particle number

As mentioned above, we also carried out a brace of tests containing 128 and 1024 particles per cloud in each phase instead of the 8192 particles of the main runs. The parameters for these simulations, dg4096 and dg512, are given in Table 1. These runs allow us to estimate the stability of our results and also to contrast them with those of Navarro & White (1993, hereafter NW93) who used 90, 368 and 1796 particles per cloud in their recent paper. They claimed that 300 particles were enough to model a collapse and obtain a crude radial profile which is not very different from that obtained with a larger number of particles. We concur with their results, but conclude that, if you want to study the formation process in detail, examining the core structure and energy transfer both between and within each of the gas and dark matter phases, then more than 1000 and possibly as many as 8000 gas particles are required.

With 128 particles even the gross properties of the collision are poorly modelled. The initial state is no longer stable and some expansion and cooling occur before the first merger. Far too much energy is dumped into the core gas during the initial collision and no subsequent reseparation takes place in the gas. The final core is huge, over 7 times as large as the one obtained in the full run. Asymptotically the gas follows the underlying dark matter which has a profile that is much steeper than that obtained in the main run. These results indicate that the conclusion of NW93, that of order 100 gas particles are required to avoid spurious energy transfers between the gas and dark matter, is over-optimistic.

A run with 1024 gas particles models the gross properties

of the collision more accurately but still has some major deficiencies. Although similar amounts of energy are transferred between the dark matter and the gas in both this and the full run (about 35 per cent in both cases, close to the 40 per cent figure of NW93), the energy is deposited into the core in the former whereas in the latter it ends up in the halo. The core gas is shocked to a much greater extent and so the core radius is larger than that formed in the full run. In the halo, the gas is hotter and has a shallower profile than the gas in run dg1.0, with a slope of 2.74 compared to 3.01. The random kinetic energy remaining in the gas is also over twice as large in this run compared to run dg1.0, revealing incomplete thermalization (this problem is even worse for run dg512 where over 20 per cent of the energy in the core gas is kinetic at the end of the simulation).

We conclude that if one wishes to model the broad properties of a collision then 1000 particles per cloud would seem to be sufficient. However, for a more detailed study examining the core properties of the gas and energy transfer between the gas and dark matter, more particles, possibly as many as 8000, are required. With fewer particles than this, more energy is transferred into the gas and a larger fraction remains as random kinetic motions at the end of the simulation. This indicates that the near-complete thermalization we obtain is not a numerical artefact.

4 DISCUSSION

4.1 Real clusters

X-ray observations of galaxy clusters have provided evidence for a core region in the gas (Jones & Forman 1984), but the interpretation of this result was complicated by the large beam size of the detectors used (see Gerbal et al. 1992). It is often assumed that the underlying gravitational potential has a core radius, as the gas sound speed is high enough to allow many crossing times in the central regions. We find that the two distributions need not be so closely related, with the central gas being shocked more than the dark matter (for which the equivalent process is phase-space mixing during the collision). The gas can then exist in hydrostatic equilibrium in the coreless potential well defined by the dark matter, whilst maintaining a constant-density core region itself.

The problem of comparing our models to the observations is complicated by the lack of a galactic population in the simulations. Although we can observe the gas via its X-ray emission, in the real world the dark matter distribution must be derived from that of the galaxies. Processes such as dynamical friction and galaxy-galaxy mergers will drive these two distribution functions apart, particularly in the dense central regions. In addition, the presence of a large central galaxy in many clusters is invariably associated with a cooling flow and may also alter the core dark matter distribution via two-body interactions.

Coupled with this, the formation of real galaxy clusters is likely to be a lot more messy than our simple mechanism, involving multi-body mergers with a range of masses, speeds and impact parameters. The colliding clusters may also contain a significant amount of substructure, with secondary infall and tidal torques providing additional complications. Preliminary results for offset mergers, to be reported in a future paper, show that a gas core is obtained for all impact parameters, formed via the same shock mechanism detailed here plus some additional rotational support.

4.2 The relative energies of the gas and dark matter

In the cores of the merger products in our simulations the gas is hotter than the dark matter, $\beta < 1$ (see equation 1). However, outside the core, throughout the majority of the cluster, we have $\beta \approx 1$. This latter result is in agreement with a previous simulation (TC92). As a consequence of this equality of specific energies for the gas and dark matter, the spatial distributions of the two phases are very similar. However, the actual form of the density profile varies in different simulations. Merger simulations (e.g. White 1980; Villumsen 1983; Paper I; this work) tend to give slopes at the half-mass radius of $s \approx 3$. More realistic simulations with continuous infall of matter give shallower slopes, $s \approx 2$ (E90; TC92).

4.3 Adding low-entropy gas

One way of eliminating the finite gas core in our simulations would be to add low-entropy gas to the cluster. This might be, for example, by the infall of cool subgroups, or by the expulsion of cold gas from galaxies. The difficulty with this is that the speeds of such systems relative to the cluster centre would in general be larger than the sound speed, and shocks would raise the entropy up to that of the cluster. For example, the slow collision considered in this paper had an initial approach speed that was equivalent to starting the clusters from rest with their centres just 2.3 cluster radii apart, and yet the core was almost as large as for the more violent collisions.

4.4 Disclaimer

We should stress that as yet no simulation of the intracluster medium has attempted to model the physical processes which must be going on within it. We know that the metallicity of the gas is about 0.3 solar and this influx of metals is associated with an unknown injection of energy. Gas and magnetic fields are continually being stripped from infalling galaxies and there is an exchange of energy between these galaxies and the gas and dark matter. We have deliberately kept our simulations simple so that the collision process can be examined in isolation. Our clusters may not, however, resemble those in the real world.

5 CONCLUSIONS

In Paper I we showed that successive collisions tend to reduce the core radii of the collisionless component as little phase vacuum is mixed into the central regions during mergers. This result holds true for the dark matter in the dual-component mergers studied in this paper.

The gas-only merger products show a small increase in core radius due to shocking of the central gas, and this effect is exaggerated in the two-phase collisions. The specific energy of the core gas is higher than that of the dark matter and so the former is more extended. At larger radii the two components have very similar profiles, close to the de Vaucouleurs profile found in Paper I (which is also approximately their initial

profile). Secondary infall may lower the slope of the density profile in real clusters (Bertschinger 1985).

The lack of any residual random kinetic energy in the gas in the central part of our simulation, in contrast to previous work, indicates that many gas particles are needed in order to model shocks correctly. SPH is a remarkably robust technique which gives surprisingly accurate results with very few particles. However, around a thousand particles per cloud are required to model a simple head-on collision in detail, and even with this number the core structure and energy transfer process are not well followed. This is an important constraint on cosmological simulations which, although they often contain many more particles *in total* than we are capable of following, also have far more elaborate structures and many more condensations, each of which consists of relatively few particles.

How generic are the results presented in this paper? We have suggested that energy is pumped from the dark matter into the gas and then irreversibly dissipated in shocks. Preliminary simulations involving off-centre collisions suggest that a similar mechanism operates in more complicated situations. Additional support of the core is provided by rotation. Our idealized models would therefore suggest a constant-density gas core region in all clusters, with a correspondingly small core radius for the underlying dark matter. Unfortunately, this conclusion neglects a wide range of physical processes as discussed above.

We believe that the combination of an adaptive high-resolution particle code and smoothed particle hydrodynamics, together with our approach of looking at relatively simple systems, has allowed us to reach new and firm conclusions about the properties of the intracluster gas in galaxy clusters and the underlying dark matter distribution.

ACKNOWLEDGMENTS

We would like to thank Simon White for a discussion on the physical mechanism of core production. PAT and HMPC acknowledge NATO Collaborative Research Grant CR6920182 which facilitated their interaction. We are grateful for use of the facilities of the STARLINK minor node at Sussex.

REFERENCES

Bertschinger E., 1985, ApJS, 58, 39
Binney J., Tremaine S., 1987, Galactic Dynamics. Princeton University Press, Princeton
Carlberg R., 1986, ApJ, 310, 593
Cavaliere A., Santangelo P., Tarquini G., Vittorio N., 1986, ApJ, 305, 651
Cen R. Y., Jameson A., Lin F., Ostriker J. P., 1990, ApJ, 326, L41
Couchman H. M. P., 1991, ApJ, 368, L23
Evrard A. E., 1990, ApJ, 363, 349 (E90)
Fabian A. C., 1991, MNRAS, 253, 29P
Gerbal D., Durret F., Lima-Neto G., Lachièze-Rey M., 1992, A&A, 253, 77
Gingold R. A., Monaghan J. J., 1977, MNRAS, 181, 375
Gingold R. A., Monaghan J. J., 1982, J. Comput. Phys., 46, 429
Hernquist L., Katz N., 1989, ApJS, 70, 419
Jones C., Forman W., 1984, ApJ, 276, 38
Katz N., White S. D. M., 1993, ApJ, 412, 455
Larson R. B., 1978, MNRAS, 184, 69
Lucy L. B., 1977, AJ, 82, 1013
Martin T. J., Pearce F. R., Thomas P. A., 1993, Preprint, University of Sussex (MPT)
Monaghan J. J., 1992, ARA&A, 30, 543
Navarro J. F., White S. D. M., 1993, MNRAS, 265, 271 (NW93)
Pearce F. R., 1992, PhD thesis, University of Sussex
Pearce F. R., Thomas P. A., Couchman H. M. P., 1993, MNRAS, 264, 497 (Paper I)
Pearce F. R., Thomas P. A., Couchman H. M. P., 1994, Preprint, University of Sussex
Sarazin C. L., 1986, Rev. Mod. Phys., 58, 1
Thomas P. A., Couchman H. M. P., 1992, MNRAS, 257, 11 (TC92)
Villumsen J. V., 1983, MNRAS, 204, 219
White S. D. M., 1980, MNRAS, 191, 1P

This paper has been produced using the Blackwell Scientific Publications LaTeX style file.